3D IDENTIFICATION OF BUILDINGS SEISMICALLY EXCITED [1]

Juan Mauricio Angeles * **Luis Alvarez-Icaza** *,[2]

* *Instituto de Ingeniería, Universidad Nacional Autónoma de México, 04510 Coyoacán DF, México*

Abstract: An algorithm to identify the parameters of a 3D model of a building subjected to two orthogonal components of seismic excitation is presented. A convenient reparameterization is proposed for a least-squares algorithm that allows an important reduction in the order of the covariance matrix, when compared with the standard formulation. This reduction facilitates real time implementation of the algorithm. Simulation results for a three stories building, that confirm analytical findings, are presented.

Keywords: Building control, parametric identification.

1. INTRODUCTION

Concern for buildings motion has increased along with their increase in height. This is specially true when external forces due to earthquakes or wind are applied to these structures. Large displacements can produce irreversible damage with traggic consequences, as those observed in Mexico City during the 1985 earthquake. There are several techniques for building motion control: active, semiactive and passive, developed to decrease the magnitude of the displacements (Connor and Klink, 1996). These techniques require the use of specialized actuators, as it is the case of magnetorheological dampers (Yang, 2001),which are devices where it is possible to control resistance to motion and are normally installed between ground and the first story of buildings (Dyke *et al.*, 1996; Jiménez Fabián, 2002; Álvarez Icaza and Jiménez, 2003; Álvarez Icaza and Carrera, 2003). To obtain good performance of the control schemes, it is convenient to have good analytical models of the buildings that accurately predict their behavior.

Civil engineers design buildings in such a way that they can withstand a design load or force for a given mass, damping and stiffness (Bazán and Meli, 1985; Meli, 1985). However, when the building is constructed, in most of the cases, real parameters are bigger that the designed ones due to several reasons, including safety factors introduced due to uncertanties. This is not a problem from the design point of view, as the real building will stand bigger loads than the design ones. For the control engineer, however, these design parameters are not fully useful to design control algorithms because their mismatch with the real parameters can deteriorate control performance. The question of how to measure the real building parameters without resorting to destructive tests is an important one. In this sense, parameter identification methods are very useful, because to use them it is only necessary to excite the structure and to measure its behavior. If excitation comes from an earthquake, identification can be done in real time and in parallel with control actions.

[1] Research supported by UNAM-DGAPA PAPIIT grant IN-110403.
[2] Corresponding author, alvar@pumas.iingen.unam.mx.

This paper deals with an efficient identification scheme that allows to obtain in real-time the parameters for a 3D building subject to two horizontal and orthogonal seismic excitation signals. The rest of the paper contains several sections that deal with the mathematical model, the identification algorithm and simulation results of the proposed scheme.

2. MATHEMATICAL MODEL

The 3D model of a shear building based on planar frames has two horizontal displacement coordinates and one horizontal torsion coordinate for each story, if the model is developed under the assumption of rigid diaphragm. The model can be derived based on the analysis of planar frames, whose interaction couple the different coordinates for all the stories of the building (Bazán and Meli, 1985; Meli, 1985; Chopra, 1995; Paz, 1997). This analysis produces a linear dynamical model that is able to predict the behavior of the building subject to external forces.

The assumption of rigid diaphragm considers that the mass of each story is concentrated and that each story behaves as a rigid body. This implies that beams in the story structure have infinite stiffness. Fig. 1 shows a scheme of a one story building with rigid diaphragm. As all points in the story have parallel motion, it is only necessary to consider 3 degrees of freedom (DOF) and therefore the stiffness matrix $K \in \mathcal{R}^{3\,X\,3}$. Any node in the diaphragm can be studied using the 3 DOF indicated in the figure.

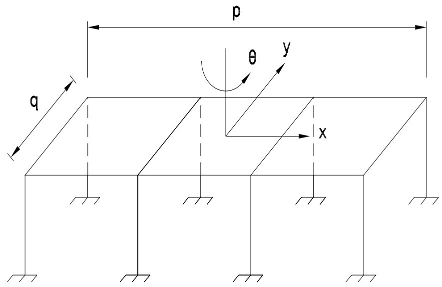

Fig. 1. Degrees of freedom of a rigid diaphragm story.

For a n stories building composed by planar frames, the stiffness matrix has a tridiagonal form as follows

$$K_d = \begin{bmatrix} k_1+k_2 & -k_2 & 0 & \cdots & 0 \\ -k_2 & k_2+k_3 & -k_3 & \cdots & 0 \\ 0 & -k_3 & k_3+k_4 & \cdots & 0 \\ \vdots & \vdots & \vdots & \ddots & \vdots \\ 0 & 0 & 0 & \cdots & k_n \end{bmatrix} > 0, \tag{1}$$

where k_i represents the stiffness of column between story i and $i-1$.

To quantify coupling between the stories and the different coordinates, it is possible to write the 3D stiffness matrix as

$$K = \begin{bmatrix} k_{xx} & k_{xy} & k_{x\theta} \\ k_{yx} & k_{yy} & k_{y\theta} \\ k_{\theta x} & k_{\theta y} & k_{\theta\theta} \end{bmatrix} \in \mathcal{R}^{3n\,x\,3n};\ K = K^T > 0, \tag{2}$$

where

$$k_{xx} = \sum_{j=1}^{f} K_{dj}\, cos^2\beta_j;\ k_{xx} = k_{xx}^T > 0,$$

$$k_{xy} = k_{yx} = \sum_{j=1}^{f} K_{dj}\, cos\beta_j\, sen\beta_j;\ k_{xy} = k_{xy}^T > 0,$$

$$k_{x\theta} = k_{\theta x} = \sum_{j=1}^{f} K_{dj}\, r_j\, cos\beta_j;\ k_{x\theta} = k_{x\theta}^T > 0,$$

$$k_{yy} = \sum_{j=1}^{f} K_{dj}\, sen^2\beta_j;\ k_{yy} = k_{yy}^T > 0,$$

$$k_{y\theta} = k_{\theta y} = \sum_{j=1}^{f} K_{dj}\, r_j\, sen\beta_j;\ k_{y\theta} = k_{y\theta}^T > 0,$$

$$k_{\theta\theta} = \sum_{j=1}^{f} K_{dj}\, r_j^2;\ k_{\theta\theta} = k_{\theta\theta}^T > 0,$$

with $k_{xx}, k_{xy}, k_{yx}, k_{x\theta}, k_{yy}, k_{y\theta}, k_{\theta y}, k_{\theta\theta} \in \mathcal{R}^{n\,x\,n}$, f the number of planar frames that compose the building, β_j the orientation of planar frame j with respect to the reference axis and K_{dj} the stiffnes of planar frame j, with form as in Eq. (1).

Damping matrix C has the same form as matrix K. Mass matrix M is given by

$$M = \begin{bmatrix} m_t & 0 & 0 \\ 0 & m_t & 0 \\ 0 & 0 & I_m \end{bmatrix} \in \mathcal{R}^{3n\,x\,3n};\ M = M^T > 0, \tag{3}$$

where

$$m_t = \sum_{j=i}^{f} m_j, \quad I_m = \left(\frac{m_t}{12}\right)(p^2+q^2),$$

with m_j the concentrated mass of frame j and p, q defined in Fig 1. Both m_t and I_m are diagonal matrices $\in \mathcal{R}^{n\,x\,n}$, therefore matrix M is also diagonal. Using these matrices, the 3D dynamical model of a building is given by (Paz, 1997)

$$M\,\ddot{U} + C\,\dot{U} + K\,U = -M\,\ddot{U}_g, \tag{4}$$

where U is the vector of displacements of each DOF, $\dot{U}$, $\ddot{U}$, are respectively their velocities and accelerations and, finally, $\ddot{U}_g$ is the acceleration of the ground, applied to all the stories.

3. PARAMETER IDENTIFICATION

Given a model structure and the values of its parameters, it is possible to obtain its response if the input is known. In many applications these parameters values can be obtained by direct measurement, applying physical laws, material properties, etc. In other applications, this is very difficult and parameters values have to be inferred by observing the response of the system for a given input. When parameters are constant or vary slowly, it is possible to use on-line parametric identification schemes, like the recursive least-squares identification scheme used in this paper (Ioannou and Sun, 1996; Åström, K.J. and Wittenmark, B., 1995; Sastry and Bodson, 1989). In the standard formulation for this method, the output of the model is expressed as the product of a regressor matrix and vector of unknown parameters. For the structure model in Eq. (4) the corresponding expression is

$$Z = \Upsilon\, \Phi, \tag{5}$$

where $Z = \ddot{U} + \ddot{U}_g$, the regressor Υ is a matrix whose elements are obtained from combinations of the elements of vectors $\dot{U}$ y U, while the parameters vector Φ contains all the non-trivial elements of $M^{-1}K$ y $M^{-1}C$. The dimensions of this matrix and vector are determined by the number of unknown parameters. If all the elements in $M^{-1}K$, $M^{-1}C \in \mathcal{R}^{3n\,x\,3n}$ were non-trivial, the total number of unknown parameters would be $18n^2$.

The least-squares algorithm to obtain an estimated $\hat{\Phi}$ of the unknown vector of parameters Φ in Eq. (5) is given by (Ioannou and Sun, 1996)

$$\dot{P} = \delta\, P - P\, \frac{\Upsilon^T\, \Upsilon}{h^2}\, P\,, \tag{6}$$

$$\dot{\hat{\Phi}} = P\, \Upsilon^T\, \varepsilon\,, \tag{7}$$

where $h^2 = 1 + \|\Upsilon\|_2^2 \in \mathcal{R}$ satisfying $\Upsilon/h \in \mathcal{L}_\infty$, $\delta > 0 \;\; \in \mathcal{R}$ is a forgetting factor, $\varepsilon = \frac{Z-\hat{Z}}{h^2} = \frac{\Upsilon\,\Phi - \Upsilon\,\hat{\Phi}}{h^2}$ is the output estimation error, $P = P^T > 0$, $P(0) > 0$ is the covariance matrix.

The dimension of the terms in Eq. (5), (6) and (7) when all the parameters are considered unknown are

$$Z \in \mathcal{R}^{3n\,x\,1},\ \Upsilon \in \mathcal{R}^{3n\,x\,18n^2},\ \Phi \in \mathcal{R}^{18n^2\,x\,1},$$
$$\varepsilon \in \mathcal{R}^{3n\,x\,1},\ P \in \mathcal{R}^{18n^2\,x\,18n^2}. \tag{8}$$

It can be noted that the order of matrix P in Eq. (8) is related with the square of the total number of DOF of the building. For the case of a 3D model, there are three DOF by story. Therefore, if the number of stories n is large, the order of matrix P can become extremely large and can have an impact on the computation time for on-line identification schemes.

In this paper, another parameterization for the dynamic model in Eq. (4) is proposed where the output is expressed by the product of a matrix Φ of unknown parameters and a regressor vector Υ, i.e., the reverse parameterization of the standard one. For this new parameterization the following results hold.

Theorem 1. Consider the system in Eq. (4), with K, C, $M \in \mathcal{R}^{q\,x\,q}$ and M a non-singular matrix with the following parameterization

$$Z = \ddot{U} + \ddot{U}_g \quad \in \mathcal{R}^{q\,x\,1},$$
$$\Phi = \begin{bmatrix} M^{-1}K & M^{-1}C \end{bmatrix} \quad \in \mathcal{R}^{q\,x\,2q},$$
$$\Upsilon = \begin{bmatrix} -U & -\dot{U} \end{bmatrix}^T \quad \in \mathcal{R}^{2q\,x\,1},$$

where Φ is the real parameters matrix such that

$$Z = \Phi\, \Upsilon. \tag{9}$$

Let $\hat{\Phi}$ be the estimated parameters matrix of the system in Eq. (4) such that

$$\hat{Z} = \hat{\Phi}\, \Upsilon. \tag{10}$$

then the algorithm given by

$$\dot{P} = \delta\, P - P\, \frac{\Upsilon\, \Upsilon^T}{h^2}\, P, \tag{11}$$

$$\dot{\hat{\Phi}}^T = P\, \Upsilon\, \varepsilon^T, \tag{12}$$

with $P = P^T > 0 \in \mathcal{R}^{2q\,x\,2q}$, $P(0) > 0$, $\delta \geq 0 \in \mathcal{R}$ a forgetting factor, $h^2 = 1 + \Upsilon^T \Upsilon \in \mathcal{R}$ satisfying $\Upsilon/h \in \mathcal{L}_\infty$ guarantees that the output estimation error

$$\varepsilon = \frac{Z - \hat{Z}}{h^2} \quad \rightarrow \quad 0 \quad \text{as} \quad t \quad \rightarrow \quad \infty$$

.

Proof: Let $\tilde{\Phi} \in \mathcal{R}^{q\,x\,2q}$ be the parameter error matrix and let $\tilde{\Phi}_r \in \mathcal{R}^{1\,x\,2q}$ be the parameter error vector corresponding with row r of matrix $\tilde{\Phi}$, i.e.,

$$\tilde{\Phi} = \Phi - \hat{\Phi} = \begin{bmatrix} \tilde{\phi}_{11} & \tilde{\phi}_{12} & \cdots & \tilde{\phi}_{1\,2q} \\ \vdots & \vdots & \ddots & \vdots \\ \tilde{\phi}_{q1} & \tilde{\phi}_{q2} & \cdots & \tilde{\phi}_{q\,2q} \end{bmatrix},$$

$$\tilde{\Phi}_r = \Phi_r - \hat{\Phi}_r = \begin{bmatrix} \tilde{\phi}_{r1} & \tilde{\phi}_{r2} & \cdots & \tilde{\phi}_{r\,2q} \end{bmatrix}. \tag{13}$$

Let $\varepsilon \in \mathcal{R}^{q\,x\,1}$ be the output estimation error vector and let $\varepsilon_r \in \mathcal{R}$ be the r element of ε corresponding to row r in Eqs. (9) and (10), i.e.,

$$\varepsilon = \frac{Z - \hat{Z}}{h^2} = \frac{\Phi\, \Upsilon - \hat{\Phi}\, \Upsilon}{h^2} = \frac{\tilde{\Phi}\, \Upsilon}{h^2},$$

$$\varepsilon_r = \frac{Z_r - \hat{Z}_r}{h^2} = \frac{\Phi_r\, \Upsilon - \hat{\Phi}_r\, \Upsilon}{h^2} = \frac{\tilde{\Phi}_r\, \Upsilon}{h^2}. \tag{14}$$

Let V be a Lyapunov candidate function

$$V = \frac{1}{h^2} \sum_{r=1}^{q} \tilde{\Phi}_r\, P^{-1}\, \tilde{\Phi}_r^T. \tag{15}$$

The time derivative of V is

$$\dot{V} = \frac{1}{h^2}\sum_{r=1}^{q} \dot{\tilde{\Phi}}_r\, P^{-1}\, \tilde{\Phi}_r^T + \frac{1}{h^2}\sum_{r=1}^{q} \tilde{\Phi}_r\, P^{-1}\, \dot{\tilde{\Phi}}_r^T + \frac{1}{h^2}\sum_{r=1}^{q} \tilde{\Phi}_r\, \dot{P}^{-1}\, \tilde{\Phi}_r^T. \quad (16)$$

Analyzing row r of $\dot{\hat{\Phi}}_r$ in Eq. (12) and substituting this in Eq. (13) and (14).

$$\dot{\tilde{\Phi}}_r^T = \dot{\Phi}_r^T - \dot{\hat{\Phi}}_r^T = 0 - P\,\Upsilon\,\varepsilon_r^T = -\frac{1}{h^2}\big(P\,\Upsilon\,\Upsilon^T\,\tilde{\Phi}_r^T\big). \quad (17)$$

Using the identity

$$P\,P^{-1} = I \quad \Rightarrow \quad \frac{d}{dt}P\,P^{-1} = \dot{P}\,P^{-1} + P\,\dot{P}^{-1} = 0$$

$$\dot{P}^{-1} = -P^{-1}\,\dot{P}\,P^{-1}.$$

From Eq. (11)

$$\dot{P}^{-1} = -P^{-1}\left(\delta P - P\frac{\Upsilon\Upsilon^T}{h^2}P\right)P^{-1}$$

$$\dot{P}^{-1} = -\delta\,P^{-1} + \frac{\Upsilon\Upsilon^T}{h^2}. \quad (18)$$

Susbtituting Eqs. (17) and (18) into Eq. (16)

$$\begin{aligned}
\dot{V} =& -\frac{1}{h^2}\sum_{r=1}^{q}\frac{1}{h^2}\tilde{\Phi}_r\Upsilon\Upsilon^T P P^{-1}\tilde{\Phi}_r^T \\
& -\frac{1}{h^2}\sum_{r=1}^{q}\frac{1}{h^2}\tilde{\Phi}_r P^{-1} P\Upsilon\,\Upsilon^T\,\tilde{\Phi}_r^T \\
& +\frac{1}{h^2}\sum_{r=1}^{q}\tilde{\Phi}_r\left(-\delta\,P^{-1} + \frac{\Upsilon\Upsilon^T}{h^2}\right)\tilde{\Phi}_r^T \\
=& -\frac{1}{h^4}\sum_{r=1}^{q}\tilde{\Phi}_r\Upsilon\Upsilon^T\tilde{\Phi}_r^T - \frac{1}{h^4}\sum_{r=1}^{q}\tilde{\Phi}_r\Upsilon\,\Upsilon^T\,\tilde{\Phi}_r^T \\
& -\frac{\delta}{h^2}\sum_{r=1}^{q}\tilde{\Phi}_r\,P^{-1}\tilde{\Phi}_r^T + \frac{1}{h^4}\sum_{r=1}^{q}\tilde{\Phi}_r\Upsilon\Upsilon^T\tilde{\Phi}_r^T \\
=& -\frac{1}{h^4}\sum_{r=1}^{q}\tilde{\Phi}_r\Upsilon\Upsilon^T\tilde{\Phi}_r^T - \frac{\delta}{h^2}\sum_{r=1}^{q}\tilde{\Phi}_r\,P^{-1}\tilde{\Phi}_r^T
\end{aligned} \quad (19)$$

Using again Eqs. (14) and (15).

$$\dot{V} = -\sum_{r=1}^{q}\varepsilon_r\,\varepsilon_r^T - \delta\,V \quad (20)$$

$$\dot{V} = -\,\varepsilon^T\,\varepsilon - \delta\,V \quad (21)$$

For the case of $\delta > 0$, it follows that $\dot{V} < 0$. This implies asymptotic stability and therefore $V \to 0$ as $t \to \infty$. When this happens, $\Phi_r \to 0$ and therefore $\varepsilon_r \to 0$, that in turn implies $\varepsilon \to 0$ (Khalil, 1996).

When $\delta = 0$ Barbalat Lemma is used. From Eq. (15) it follows that V is bounded from below and from Eq. (21) that $\dot{V}$ is negative semi-definite, if $\delta = 0$. Finally, as $\dot{V}$ is uniformly continuous because its time derivative is bounded, then

$$\dot{V} = -\,\varepsilon^T\varepsilon \quad \to 0 \qquad \text{as} \qquad t \to \infty$$

$\dot{V} \to 0$ implies $\varepsilon \to 0$, that guarantees that the estimated output $\hat{Z}$ is equal to the real output. For the case of $\delta = 0$ persistence of excitation is required to guarantee that $\tilde{\theta} = 0$. □

For the system in Eq. (4) where $M^{-1}K$, $M^{-1}C \in \mathcal{R}^{3n\,x\,3n}$, the order of the terms in the parameterization in Eq. (9) and in the least-squares algorithm in Eqs. (11)-(12) is

$$Z \in \mathcal{R}^{3n\,x\,1},\ \Upsilon \in \mathcal{R}^{6n\,x\,1},\ \Phi \in \mathcal{R}^{3n\,x\,6n},\ \varepsilon \in \mathcal{R}^{3n\,x\,1},\ P \in \mathcal{R}^{6n\,x\,6n} \quad (22)$$

It is clear that the order of matrix P en Eq. (22) is smaller than the order of the same matrix in Eq. (8), that is used in the standard least-squares parameterization. This reduction is very convenient as is related directly to the computing time. There is another size reduction in the regressor Υ that has also a positive influence from the persistence of excitation point of view. The smaller the size of this regressor, the easier to satisfy persistence of excitation conditions.

4. SIMULATION RESULTS

To simulate the least-squares identification algorithm in Theorem 1, a three story building model was used. This building is formed by 4 planar frames as shown in Fig. 2. The values for the mass, damping and stiffness matrices were obtained from a similar planar small size model (Jiménez Fabián, 2002). The values for the elements of these matrices are shown in Table **??**.

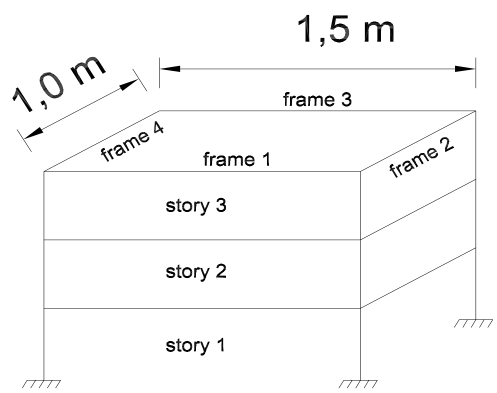

Fig. 2. Building used for simulations.

The seismic excitation signal used for the simulations came from two records taken at "Secretaría de Comunicaciones y Transportes" (SCT) during

Table 1 Nominal parameters for the model used in simulations

parameters	story	frame 1	frame 2	frame 3	frame 4
	1	98,3	94,5	95,3	97,8
m $[kg]$	2	97,5	95,8	94,6	98,4
	3	92,5	94,0	96,3	94,9
	1	120	119	117	122
c $\left[\frac{N\,s}{m}\right]$	2	124	123	125	127
	3	125	123	128	124
	1	5,16	4,84	6,01	6,04
k $\left[\frac{N}{m}\right](10^5)$	2	4,48	4,99	5,87	5,23
	3	5,89	5,78	5,46	5,12

an earthquake that occurred at Mexico City on September 19th, 1985. Figs. 3 and 4 show the records of the orthogonal horizontal accelerations. Although the earthquake lasted for 180 seconds, the simulation results refer only to the first 4 seconds of the earthquake, as convergence was obtained before this time and after it there is not significant change in the parameters value. Initial condition for covariance matrix P and forgetting factor are

$$P(0) = \begin{bmatrix} 10^{19}\, I_9 & 0_9 \\ 0_9 & 10^{14}\, I_9 \end{bmatrix}; \qquad \delta = 0,01$$

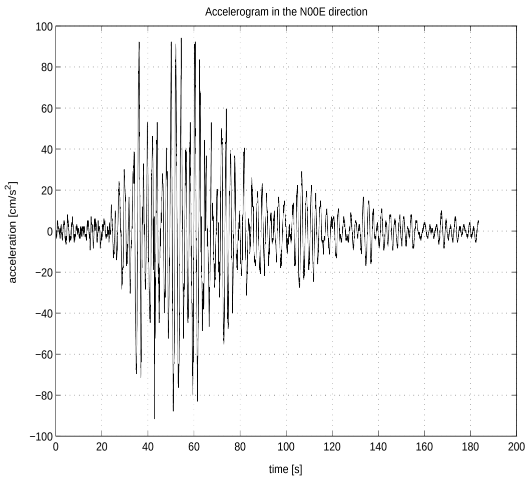

Fig. 3. Acceleration of the earthquake at SCT in N00E direction.

To show the performance of the least-squares algorithm in Eqs. (11) - (12), Fig. 5 shows the output estimation error norm $\|\varepsilon\|_2$. It can be noted in Fig. 5 that $\|\varepsilon\|_2$ decreases with time, confirming asymptotic stability. Figs. 6 and 7 show two examples of parameter identification time evolution, one of them related with stiffness and the other with damping.

Fig. 8 shows the real and estimated accelerations, the outputs of the system in this case, for the three DOF of the first story. Due to the good convergence obtained, the difference between the two curves can not be noted.

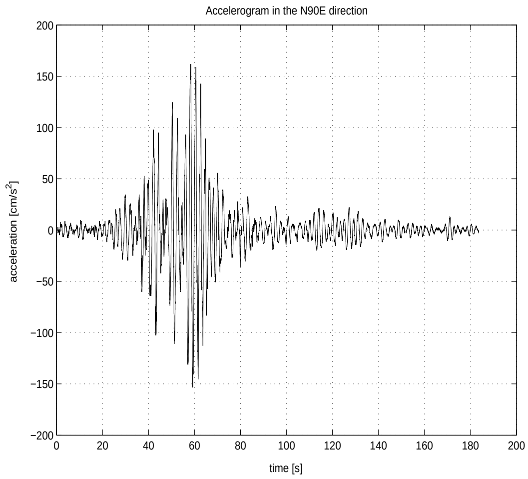

Fig. 4. Acceleration of the earthquake at SCT in N00E direction.

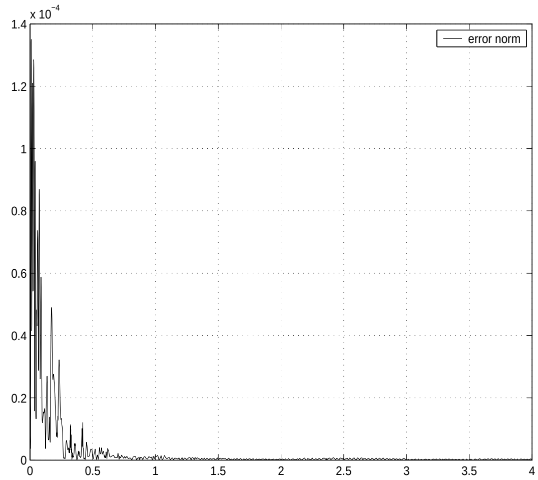

Fig. 5. Output estimation error norm: $\|\varepsilon\|_2$.

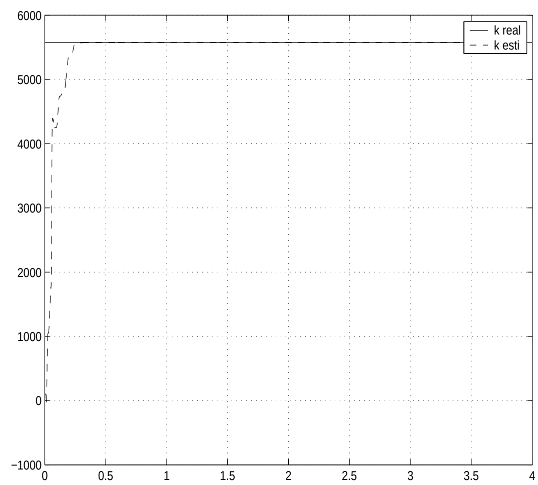

Fig. 6. Time evolution of identification of element $(M^{-1}K)_{1,1}$.

The simulation results here presented did not include the effect of noise. When noise in the level found in accelerometers is added, estimation of parameters and accelerations remains very good.

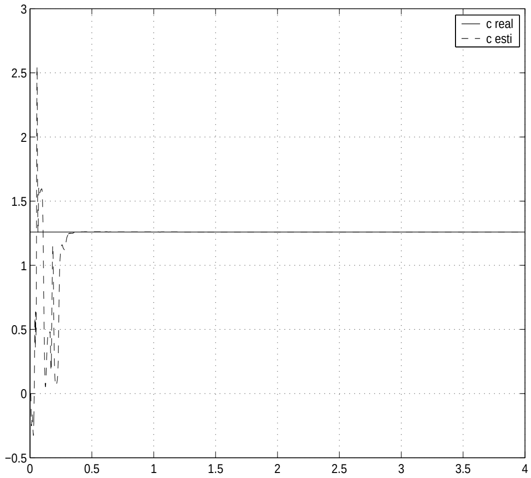

Fig. 7. Time evolution of identification of element $(M^{-1}C)_{1,1}$.

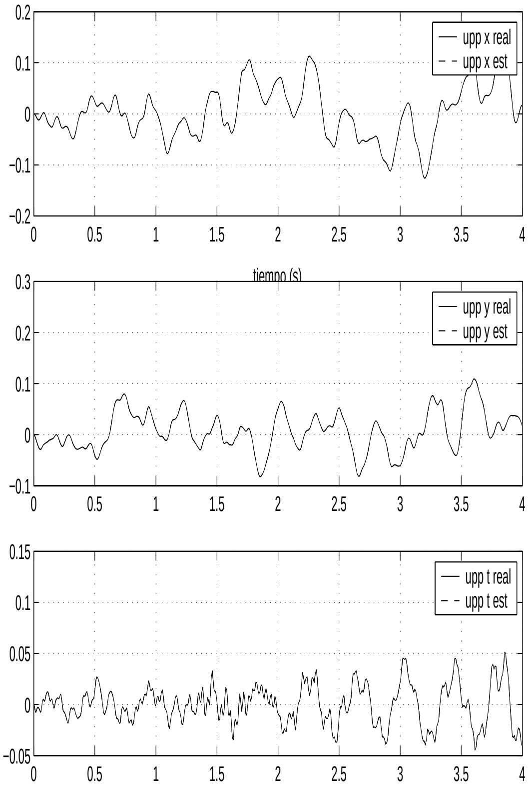

Fig. 8. Real and estimated acceleration, 3 DOF of the first story.

5. CONCLUSION

A least-squares algorithm for the identification of the parameters of a 3D linear building model was presented. The algorithm introduces a new parameterization that allows substantial reductions in the order of the covariance matrix and facilites fulfilling of the persistence of excitation condition. Although the analysis was developed for a shear building, the algorithm can be used in other applications where a story is divided into a finite number of nodes. Simulation results were presented that confirm analytical findings.

REFERENCES

Álvarez Icaza, L. and R. Carrera (2003). Control de estructuras civiles con modulación en frecuencia. In: *Memorias del Congreso Nacional de Control Automático*. Vol. 970-32-1173-9. pp. 372–377.

Álvarez Icaza, L. and R. Jiménez (2003). Observador adaptable para el control de estructuras civiles. In: *Memorias del Congreso Nacional de Control Automático*. Vol. 970-32-1173-9. pp. 360–365.

Bazán, E. and R. Meli (1985). *Manual de diseño sísmico de edificios*. Limusa.

Chopra, A.K. (1995). *Dynamics of Structures: Theory and Applications to Earthquake Engineering*. Prentice-Hall. Upper Saddle River, NJ.

Connor, J. J. and B. S. A. Klink (1996). *Introduction to motion based design*. Computational Mechanics. Southampton, United Kingdom.

Dyke, S.J., B.F. Spencer, M.K. Sain and J.D. Carlson (1996). Seismic response reduction using magnetorheological dampers. In: *Proceedings of the 1996 IFAC World Congress, San Francisco*. Vol. L. pp. 145–150.

Ioannou, P.A. and J. Sun (1996). *Robust Adaptive Control*. Prentice-Hall. Upper Saddle River, NJ.

Jiménez Fabián, René Enrique (2002). Control semiactivo de estructuras civiles usando amortiguadores magneto-reológicos. Master Thesis. Programa de Maestría y Doctorado en Ingeniería, Universidad Nacional Autónoma de México.

Khalil, H. K. (1996). *Nonlinear Systems*. 2nd ed. Pretice Hall. Upper Saddle River, NJ.

Meli, R. (1985). *Diseño estructural*. Limusa.

Åström, K.J. and Wittenmark, B. (1995). *Adaptive Control*. 2nd ed. Addison-Wesley. USA.

Paz, M. (1997). *Structural Dynamics: theory and computation*. 4th. ed. Chapman & Hall, International Thomson Publishing. New York, NY.

Sastry, S. and M. Bodson (1989). *Adaptive control: stability, convergence and robustness*. Prentice-Hall. Upper Saddle River, NJ.

Yang, G. (2001). Large-sacle magnetorheological fluid damper for mitigation: modeling, testing and control. PhD thesis. Departament of Civil Engineering and Geological Sciences. Notre Dame, Indiana, USA.